Progress In Electromagnetics Research C, Vol. 29, 17–28, 2012

RECTANGULAR STEPPED PATCH ANTENNA AT GSM 900 FOR ENERGY SCAVENGING

N. Md. Din[1], C. K. Chakrabarty[1], K. K. A. Devi[2,*], and S. Sadasivam[2]

[1]Department of Electronics and Communication Engineering, Universiti Tenaga Nasional, Putrajaya Campus, Kajang 43000, Malaysia

[2]Department of Electrical and Electronic Engineering, INTI International University, Nilai 71800, Malaysia

Abstract—This paper presents a novel 377 Ω rectangular stepped patch antenna with partial ground plane at downlink radio frequency range of GSM-900 band. Two steps are incorporated into the patch antenna, and bandwidth expansion was investigated by the currents flowing through the patch antenna. The antenna simulation was carried out in the ADS 2009 environment. The fabricated antenna on FR4 substrate indicates an impedance bandwidth of 32.7% (310 MHz) at 947 MHz centre frequency with return loss of −28.12 dB. The simulated, test and field results of the antenna design are discussed.

1. INTRODUCTION

Patch antennas offer effective low-profile designs for a wide range of wireless applications. They are inexpensive to fabricate, light in weight, suitable for high frequency applications and support multiple function circuits. But they have a main shortcoming of narrow bandwidth. This problem has been addressed by researchers and many configurations have been proposed for bandwidth enhancement.

In [1], authors provided an effect on bandwidth using variation in substrate thickness and its permittivity, and showed that erratic result was obtained for substrates thicker than about $0.02\lambda_0$. While introducing U shaped slot in the rectangular patch was able to achieve an impedance bandwidth of 10–40% in [2]. The impedance bandwidth was enhanced to 44% by increasing the thickness of the substrate

Received 2 March 2012, Accepted 17 April 2012, Scheduled 21 April 2012

* Corresponding author: Kavuri Kasi Annapurna Devi (kavurik.adevi@newinti.edu.my).

by the addition of second U slot over the main U shaped patch in [3]. The technique of L shaped probe feed implemented on a thick substrate achieved an impedance bandwidth of 30.3% at the frequency range of 1.9 to 2.4 GHz in [4]. A rectangular micro strip antenna with a foam layer thickness of around 10% of the wavelength using L shaped probe feed achieved an impedance bandwidth of 35% at frequency range of 3.76–5.44 GHz in [5]. Three different types of feeding techniques were employed at the centre frequency of 3.3 GHz and able to achieve an impedance bandwidth in the range of 17.1-24% in [6]. Chip resistor loading technique was implemented in [7] and achieved an impedance bandwidth 9.3% at the centre frequency of 710 MHz. Authors in [8] used two U-shaped parasitic elements along the radiating edges of a probe fed rectangular patch antenna to achieve the impedance bandwidth of 27.3% at the centre frequency of 5.5 GHz. In [9], an impedance bandwidth of 22% at 5 GHz centre frequency was obtained using an unequal patch sizes and without an air region separation on the triple patch antennas. A half U-slot patch antenna with shorting pin technique achieved an impedance bandwidth of 20% at 900 MHz centre frequency and a half E-shaped patch antenna obtained an impedance bandwidth of 25.2% at 2.57 GHz centre frequency in [10]. The design in [11] combined the wideband U-slot and L-probe-fed patch with the addition of a shorting wall and shorting pin techniques, obtained an impedance bandwidth of 20% at 3.755 GHz centre frequency. In [12] proposed two closely staggered resonant modes to achieve an impedance bandwidth of 13.3% at 900 MHz centre frequency using two unequal arms of the U-shaped patch. In [13] the impedance bandwidth of 19.8% at 2.378 GHz centre frequency was obtained using shorted wall loading and introducing multi resonance in the low profile E shaped patch antenna. In [14], broadband impedance matching was proposed using Fano's theory where an impedance bandwidth of 12% at 3.34 GHz centre frequency was obtained. In [15], authors implemented a square patch antenna with a cross shaped slot on the surface through an aperture coupling. The design achieved a return loss S_{11} of -14 dB at 2.45 GHz.

In this paper, a novel stepped patch antenna is designed for 377 Ω impedance with partial ground plane, which operates in the impedance bandwidth range of 845 MHz to 1160 MHz (315 MHz). This accomplishes the purpose of wideband antenna for RF energy harvesting at GSM-900 downlink radio frequency band. The discerning features of this designed antenna is in the impedance of the antenna, matching network design, ground plane technique and frequency of operation (GSM-900 downlink frequency band) which all differs from the previous works described.

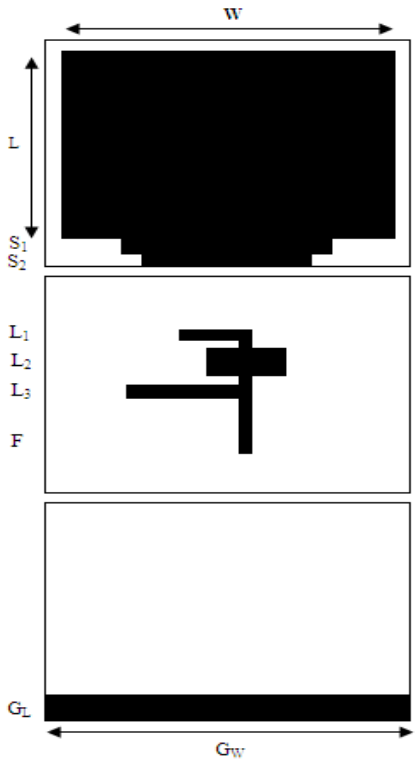

Figure 1. Basic configuration of stepped patch antenna with Pi matching network and partial ground.

Section 2 describes the design of antenna and the matching network. Section 3 describes the procedure of measurements carried out. Section 4 discusses both simulated and measured results of the antenna performance. Finally, the paper is concluded in Section 5 with the findings of the simulated and measured results.

2. ANTENNA AND PI MATCHING NETWORK DESIGN

The antenna design for wide band 377 Ω stepped patch antenna with partial ground plane is shown in Figure 1. The topology of antenna is designed on an FR4 substrate with 1.6 mm thickness and dielectric constant of 3.9. The antenna consists of a larger patch, followed by a larger step, smaller step, Pi matching network, a smaller patch which serves as the feed line and a partial ground plane.

The patch antenna's basic width and length are denoted by 'W' and 'L' are formalized [16] by the Equations (1) and (2)

$$W = \frac{1}{2f_r\sqrt{\mu_0\epsilon_0}}\sqrt{\frac{2}{\epsilon_r+1}} = \frac{v_0}{2f_r}\sqrt{\frac{2}{\epsilon_r+1}} \tag{1}$$

$$L = \frac{\lambda}{2} - \Delta L = \frac{1}{2f_r\sqrt{\epsilon_{reff}}\sqrt{\mu_0\epsilon_0}} - 2\Delta L \tag{2}$$

The two steps on the patch antenna are denoted by 'S_1' and 'S_2'. The three components of the pi matching network are represented by L_1, L_2 and L_3 respectively. The feed line is denoted by F. The structure of the stepped patch antenna and the pi matching network is printed on one side of the FR4 substrate with the partial ground plane on the other side. The partial ground plane width and length are denoted by 'G_L' and 'G_W' as shown in Figure 1. The design parameters such as dimensions (length and width) of patch, steps, pi matching network, the feedline and the partial ground plane are optimized to obtain the better return loss and wide impedance bandwidth. The optimized dimensions of the antenna structure are as shown in Table 1.

The geometry has a discontinuity which is denoted by the steps S_1 and S_2 at the bottom edge of the patch antenna. The existence of these steps provides the different resonant frequencies in the specified frequency band. The change in the resonant frequency is due to the role played by various factors such as step dimension, position, matching network design, position, feed line and the partial ground plane. This causes a change in electric and magnetic field distributions near the discontinuities. The altered electric field distribution exhibits a change in the capacitance and the change in magnetic field distribution presents in terms of equivalent inductance. Figure 2 shows the capacitance and inductance of the equivalent circuit for steps 'S_1' and 'S_2' of the patch antenna.

Figure 2(b) is the representation of the steps width W_1 and W_2. From [17] it has been shown that the steps in the structure will increase the bandwidth. This is because each step mimics a resonance patch

Table 1. Dimensions of antenna geometry.

Basic Configuration	Patch antenna						Pi Matching Network						Feed Line		Ground Plane	
Variable	W	L	S_1		S_2		L_1		L_2		L_3					
			W	L	W	L	W	L	W	L	W	L	W	L	W	L
Dimensions	59	79.4	4.5	49	3.5	39	3	11	12	8	19	9	10	3	3	80.2

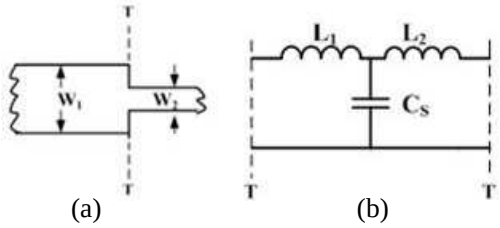

Figure 2. (a) Micro strip step discontinuity, (b) equivalent circuit.

at the desired frequency. When these steps are cascaded the resulting bandwidth of antenna structure will be increased.

The pi matching network in the geometry was designed to provide a good impedance match for the antenna 377 Ω impedance to the measuring device impedance 50 Ω to transform maximum power from the antenna to the load (50 Ω measuring device). The output of the pi matching network is connected to the 50 Ω SMA connector through a micro strip feed line. SMA connector was used for the coaxial-to-micro strip transition, connecting the antenna to the network analyzer. The design starts off with the lumped elements model where by the matching network have shunt open circuit capacitors and a series inductor. The lumped elements in the matching network are then transformed into distributed elements to obtain the initial values of length and width for each distributed component using the Equations (3) to (5). By using ADS the optimized dimensions of the distributed elements in the matching network were obtained.

$$Z_{\text{in}}^{oc} = -jZ_0 \cot \beta\ell = -j50 \cot \beta\ell \tag{3}$$

where $\beta = \frac{2\pi}{\lambda}$ and $\lambda = \frac{\lambda_0}{\sqrt{\varepsilon_{reff}}}$

$$Z_{\text{capce}}^{oc} = \frac{1}{j\omega C} \tag{4}$$

$$Z_{\text{indct}}^{oc} = j\omega L \tag{5}$$

The center conductor pin of SMA connector was soldered to the micro strip feed line and ground plane. The effect of ground plane is the vital factor in the present design of antenna for the required application. A finite analysis was carried out on the ground plane and the currents are calculated to realize which areas of antenna are effective for the required operation. This result made to choose the partial ground plane with the dimension of 80 mm × 3 mm which is about 20 times less that of the size of the patch antenna using the technique developed in [18].

3. METHODOLOGY

The properties and performance of the antenna have been predicted and optimized through electromagnetic simulation software in Agilent ADS 2009 environment [19]. The method of moments (MoM) was used for analysis and the Green's vector function was chosen as the basis function to demonstrate the performance of the wide band configuration. The characteristics of the fabricated antenna have been measured using the Advantest R3767CG network analyzer.

The far field radiation measurement was carried out using two fabricated antennas from a known signal source, at an open space to prevent the reflections from the walls. One antenna was integrated with the signal source as a transmitting antenna; the other is integrated with the spectrum analyzer Advantest U3751, which was arranged on a rotating machine to rotate 360 degree (0 degree to 360 degrees). In order to ensure the presence of far field region the distance between the two antennas was maintained at 100 cm throughout the rotation. The power levels recorded for three test frequencies 957 MHz, 945 MHz and 936 MHz for downlink radio frequency of GSM-900 band.

4. RESULTS AND DISCUSSION

The picture of fabricated stepped patch antenna on an FR4 substrate is shown in Figure 3. The simulated and measured return loss obtained results for the antenna is shown in Figure 4. In simulation, return loss -33.41 dB at resonant frequency 943 MHz and in the test -28.12 dB at 947 MHz resonant frequency was achieved. The frequency band ranges from 852 MHz to 1162 MHz (310 MHz) provides an impedance bandwidth of 32.7% at 947 MHz. The summarized results are shown in Table 2. The analysis shows that the simulated result of return loss complies with the test return loss below -10 dB throughout the impedance bandwidth, which clearly shows that the antenna is well suited for downlink radio frequency range of GSM-900 band application.

Table 2. Simulation and test performance.

Results	At -10 dB f_l and f_h Frequency (MHz)	Impedance Bandwidth (MHz)	Return loss (dB)
Simulation	827 and 1100	273 (28.9%@943)	-33.41 (943 MHz)
Test	852 and 1162	310 (32.7%@947)	-28.12 (947 MHz)

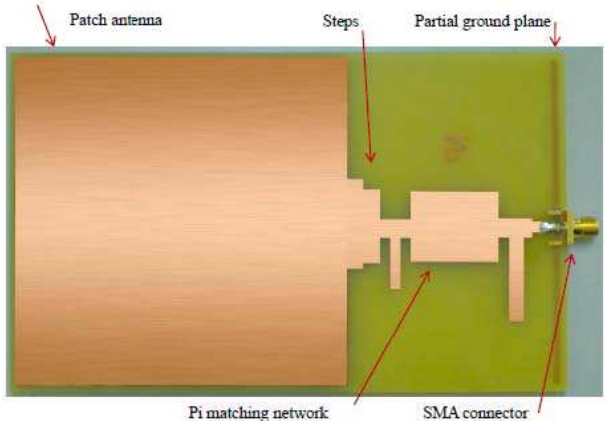

Figure 3. Picture of fabricated stepped patch antenna.

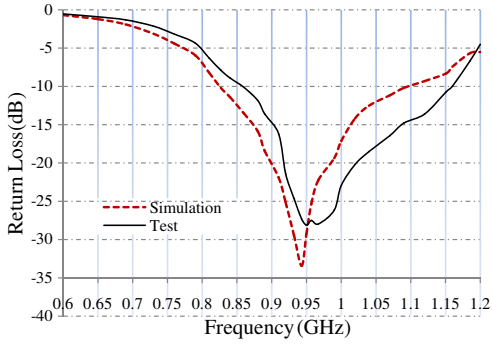

Figure 4. Simulated and measured results of return loss (dB) against frequency (GHz).

The currents flowing through the designed antenna at three test frequencies 957 MHz, 945 MHz, and 936 MHz of down link band in Agilent ADS environment is shown in Figure 5. The current density around steps S_1 and S_2 and along the radiating edges of the patch is shown to be higher at 957 MHz and 945 MHz. And as such these antennas behave like an array of two in-phase monopoles whereby the radiation pattern is expected to have prominent side lobes. Whereas for the frequency at 936 MHz, the current distribution throughout the patch is mostly uniform with only a slight increase at the edges. The radiation pattern is expected to be weaker with lower strength level of the main lobes as compared with at frequencies 945 MHz and 957 MHz.

In order to validate the modeled current densities, the far field radiation pattern was measured for the three test frequencies in the

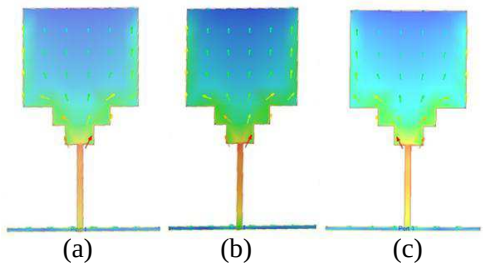

Figure 5. Simulated currents distribution at (a) 957 MHz, (b) 945 MHz, (c) 936 MHz.

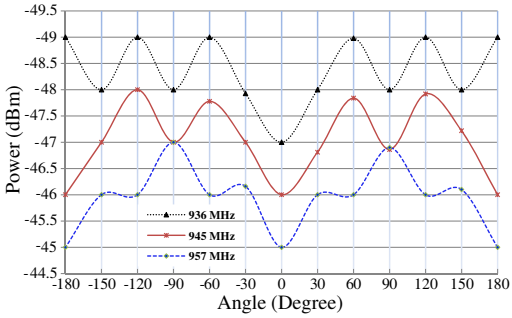

Figure 6. Measured radiation pattern.

downlink radio frequency range of GSM-900 band shown in Figure 6. From the figure it is observed that for all test frequencies 957 MHz, 945 MHz and 936 MHz, the amplitude of power distribution pattern consists of main lobe at 0 degree and 1st minor lobes at ± 90 degree. The reason for the presence of side lobes in the measured radiation pattern has been justified from the current density profile shown in Figure 5. From the measured far field radiation patterns and simulated current density profiles, the test antennas clearly behaves as an array of two in-phase monopoles whereby the fundamental lobe lies along the axis of the patch. This shows that the radiation pattern agrees with the result of current distribution shown in Figure 5 and the enhancement of the bandwidth in the frequency band is contributed by both step 1 and 2 of the antenna.

Figure 7 shows the normalized model and measured antenna impedances for the down link frequency band. The model and the measured antenna impedances on the graph are found to be close and overlapped in the desired frequency band. It is observed that the model and measured reactive components are sensitive to the frequency

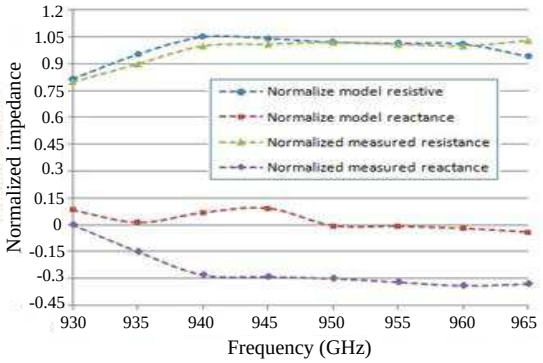

Figure 7. Normalized impedances versus frequency.

variation in the band and the dimensions of the antenna. From this analysis, it is evident that the antenna designed is providing a perfect match for both model and measured impedances and it is well suited to capture the ambient RF energy at the downlink radio frequency range of GSM-900 band.

From the results and analysis of radiation pattern and the normalized impedance graphs shown in Figures 6 and 7, it is clearly justified that the proposed antenna quiet well matched to the free space impedance. This is the reason behind the maximum flow of current at the matched frequency band as shown in Figure 5.

Based on the best results obtained, the antenna was proposed to carry out the outdoor field trial in the vicinity of GSM and UTMS cell tower at a distance of 400 m with close line of sight and the captured spectrum is shown in Figure 8. The test frequency was set with the start frequency 890 MHz which is almost equal to the GSM-900 uplink start frequency (uplink band 890.2–914.8 MHz), the end frequency of 970 MHz was set, which is beyond the GSM-900 downlink frequency band (935.2 MHz–959.8 MHz). Even though the proposed antenna was designed for GSM downlink band, these experimental frequencies were set in the spectrum analyzer in order to test the performance of the antenna in both uplink and downlink frequencies. From the spectrum figure, it is vividly shown that the antenna started capturing signals from 936 MHz to 957.98 MHz which is strictly falling under the GSM-900 downlink band and the spectrum shows only the noise level of -70 dBm beyond this frequency band. The peak signal level -25.59 dBm (2.75 μW) was observed at 957.98 MHz. The high power level captured clearly shows that the 377 Ω impedance of the designed antenna matches closely with the free space impedance 377 Ω.

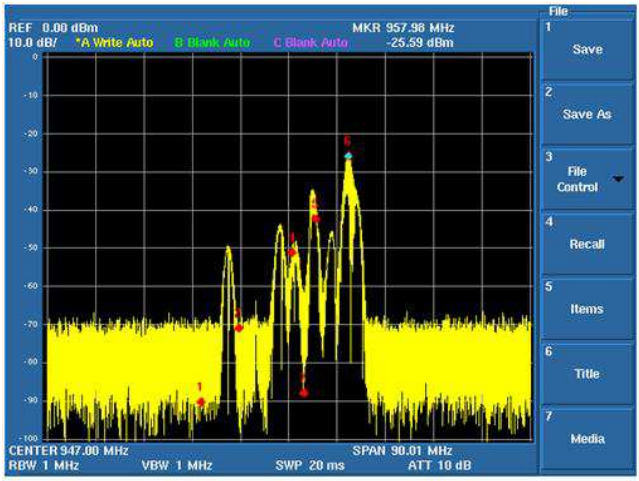

Figure 8. Antenna field measurement spectrum at GSM-900.

5. CONCLUSIONS

The rectangular stepped patch antenna with wide bandwidth is presented in this paper. Compared to the established performance characteristics of the wide band micro strip patch antennas, the presented antenna has a novel feature of achieving a wide impedance bandwidth for matching to a free space impedance 377 Ω, also a simple design and small in size. The antenna geometry, return loss, current density through the patch, measured radiation pattern, model and measured normalized impedances and field test results of the antenna are presented. This shows that the proposed antenna has all the capabilities for use in energy harvester at GSM-900 downlink frequency band.

ACKNOWLEDGMENT

We would like to acknowledge and thank the Ministry of Higher Education Malaysia for funding this project under the Fundamental Research Grant FRGS/1/10/TK/UNITEN/02/13.

REFERENCES

1. Schaubert, D. H., D. M. Pozar, and A. Adrian, "Effect of microstrip antenna substrate thickness and permittivity:

Comparison of theories and experiment," *IEEE Trans. on Antennas and Propag.*, Vol. 37, 677–682, Jun. 1989.

2. Huynh, T. and K. F. Lee, "Single-layer single-patch wide band microstrip antenna," *Electron. Lett.*, Vol. 31, 1310–1312, 1995.
3. Guo, Y. X., K. M. Luk, K. F. Lee, and Y. L. Chow, "Double U-slot rectangular patch antenna," *Electron. Lett.*, Vol. 34, 1805–1806, 1998.
4. Yang, F., X.-X. Zhang, X. Ye, and Y. Rahmat-Samii, "Wide-band E shaped patch antennas for wireless communications," *IEEE Trans. on Antennas and Propag.*, Vol. 49, 1094–1100, Jul. 2001.
5. Luk, K. M., C. L. Mak, Y. L. Chow, and K. F. Lee, "Broadband microstrip patch antenna," *Electron. Lett.*, Vol. 34, 1442–1443, Jul. 1998.
6. Kumar, G. and K. C. Gupta, "Directly coupled multiple resonator wide-band microstrip antenna," *IEEE Trans. on Antennas and Propag.*, Vol. 33, 588–593, Jun. 1985.
7. Wong, K. L. and Y. F. Lin, "Small broadband rectangular microstrip antenna with chip-resistor loading," *Electron. Lett.*, Vol. 39, 1593–1594, 1997.
8. Wi, S. H., Y. S. Lee, and J. G. Yook, "Wideband microstrip patch antenna with U-shaped parasitic elements," *IEEE Trans. on Antennas and Propag.*, Vol. 55, No. 4, Apr. 2007.
9. Bulja, S. and D. M. Syahkal, "Broadband microstrip antennas using unequal patches," *IEEE Antennas and Propagation Society International Symposium*, 3731–3734, Jul. 2006.
10. Chair, R., C.-L. Mak, K.-F. Lee, K.-M. Luk, and A. A. Kishk, "Miniature wide-band half U-slot and half E-shaped patch antennas," *IEEE Trans. on Antennas and Propag.*, Vol. 53, 2645–2652, Aug. 2005.
11. Shackelford, A. K., K.-F. Lee, and K. M. Luk, "Design of small-size wide-bandwidth micro-strip patch antennas," *IEEE Antennas Propag. Mag.*, Vol. 45, No. 1, 75–83, Feb. 2003.
12. Guo, Y.-X., K.-M. Luk, K.-F. Lee, and R. Chair, "A quarter-wave U-shaped antenna with two unequal arms for wideband and dual-frequency operation," *IEEE Trans. on Antennas and Propag.*, Vol. 50, 1082–1087, Aug. 2002.
13. Xiong, J., Z. Ying, and S. He, "A broadband E-shaped patch antenna of compact size and low profile," *IEEE Antennas and Propagation Society International Symposium*, 1–4, Jul. 2008.
14. Pues, H. F. and A. R. Van De Capelle, "An impedance matching technique for increasing the bandwidth of microstrip antennas,"

IEEE Trans. on Antennas and Propag., Vol. 37, No. 11, 1345–1354, Nov. 1989.

15. Vera, G. A., A. Georgiadis, A. Collado, and S. Via, "Design of a 2.45 GHz rectenna for electromagnetic (EM) energy scavenging," *IEEE Radio and Wireless Symposium*, 61–64, Mar. 2010.
16. Balanis, C. A., *Antenna Theory: Analysis and Design*, John Wiley & Sons, Newyork, 2005.
17. Badjian, M. H., C. K. Chakrabarty, S. Devkumar, and G. C. Hock, "Circuit modeling of an UWB patch antenna," *International RF & Microwave Conference*, 3–6, Apr. 2009.
18. Garg, R., P. Bhartia, I. Bahl, and A. Ittipiboon, *Microstrip Antenna Design Handbook*, 534–538, Artech House, Boston, London, 2001.
19. ADS, *User Manual*, Agilent Technologies Ltd, USA, 2008.